

Improving the phenomenology of $K_{\ell 3}$ form factors with analyticity and unitarity

Gauhar Abbas,¹ B.Ananthanarayan,¹ Irinel Caprini,² and I. Sentitemsu Imsong¹

¹*Centre for High Energy Physics, Indian Institute of Science, Bangalore 560 012, India*

²*National Institute of Physics and Nuclear Engineering
POB MG 6, Bucharest, R-76900, Romania*

The shape of the vector and scalar $K_{\ell 3}$ form factors is investigated by exploiting analyticity and unitarity in a model-independent formalism. The method uses as input dispersion relations for certain correlators computed in perturbative QCD in the deep Euclidean region, soft-meson theorems, and experimental information on the phase and modulus of the form factors along the elastic part of the unitarity cut. We derive constraints on the coefficients of the parameterizations valid in the semileptonic range and on the truncation error. The method also predicts low-energy domains in the complex t -plane where zeros of the form factors are excluded. The results are useful for $K_{\ell 3}$ data analyses and provide theoretical underpinning for recent phenomenological dispersive representations for the form factors.

PACS numbers: 11.55.Fv, 13.20.Eb, 11.30Rd

I. INTRODUCTION

$K_{\ell 3}$ decays, along with the leptonic decay of the kaon, are the gold-plated channels for a precise determination of $|V_{us}|$, where V_{us} is the element of the Cabibbo-Kobayashi-Maskawa matrix (for recent reviews see [1]-[5]). The amplitude of the process involves the matrix element of the strangeness-changing vector current between a kaon and a pion, written as:

$$\begin{aligned} \langle \pi^0(p') | \bar{s} \gamma_\mu u | K^+(p) \rangle \\ = \frac{1}{\sqrt{2}} [(p' + p)_\mu f_+(t) + (p - p')_\mu f_-(t)], \end{aligned} \quad (1)$$

where $f_+(t)$ is the vector form factor and the combination

$$f_0(t) = f_+(t) + \frac{t}{M_K^2 - M_\pi^2} f_-(t) \quad (2)$$

is known as the scalar form factor. The matrix element for the charged pion and the neutral kaon is related to (2) by isospin symmetry.

The $K_{\ell 3}$ decay rates were measured for the four modes ($K = K^\pm, K^0$ and $\ell = \mu, e$) by several experimental groups [6]-[15]. The rates are conveniently written as

$$\Gamma_{K_{\ell 3}} = \frac{G_F^2 M_K^5}{192\pi^3} C_K^2 S_{EW} \left| f_+(0) V_{us} \right|^2 I_K^\ell (1 + \Delta), \quad (3)$$

where G_F is the Fermi constant, C_K is the Clebsch-Gordan coefficient equal to 1 ($1/\sqrt{2}$) for the neutral (charged) kaon decays, S_{EW} is a short-distance electroweak correction, and Δ accounts for the electromagnetic and isospin-breaking corrections. The form factors enter through the value $f_+(0)$ at zero momentum transfer and the phase space integral I_K^ℓ , which depends on the shape of the form factors in the physical range $M_\ell^2 \leq t \leq (M_K - M_\pi)^2$.

For a precise determination of $|V_{us}|$, it is important to improve the accuracy of the parameterizations of the

form factors using additional theoretical and experimental information. Thus, the low-energy theorems based on chiral symmetry provide values of the form factors at some special points inside the analyticity domain [16]-[21]. On the unitarity cut, which extends from $t_+ = (M_K + M_\pi)^2$ to ∞ , the Fermi-Watson theorem [22, 23] implies that, below the inelastic threshold t_{in} , the phase is available from the corresponding partial wave of pion-kaon elastic scattering. Furthermore, recent measurements of $\tau \rightarrow K\pi\nu_\tau$ decays [24] provide experimental information also on the modulus in the same region.

Analyticity is the ideal tool for relating the information from the unitarity cut to the semileptonic range. Several comprehensive dispersive analyses were performed recently, using either coupled channels Muskhelishvili - Omnès equations [25]-[28] or a single-channel Omnès representation [29, 30]. The dispersive representations can be extrapolated below the cut, providing information on the shape of the form factors in the $K_{\ell 3}$ region. However, direct applications of the dispersion relation for the data analysis are not usual, although exceptions are the Omnès-type relations [29, 30], used recently in the data analyses by NA48 [12], KLOE [13] and KTeV [14] Collaborations. Such an analysis of BELLE data for τ decays that probe the vector form factor is found in [31].

The purpose of the present paper is to discuss the implications of analyticity for the phenomenological analyses using an alternative approach proposed some years ago [32-34], known as the method of unitarity bounds. We use the fact that a bound on an integral involving the modulus squared of the form factors along the unitarity cut is known from the dispersion relation satisfied by a certain QCD correlator. Standard mathematical techniques then allow one to correlate the values of the form factor or its derivative at different points. For the $K\pi$ form factors, the method was applied in [35-41]. The latest applications [40, 41] led, in particular, to stringent constraints on the shape of the scalar form factor at low energies.

In the present work, we consider both the vector and

the scalar form factors and focus on the phenomenological consequences of analyticity and unitarity for $K_{\ell 3}$ analyses. One of our aims is to present simple analytic constraints, easily implementable in phenomenological studies, on the free coefficients of the parameterizations used in fitting the data. In contrast to other recent works, the present work does not require any input about the absence of zeros on the real energy line or in the complex energy plane, nor does it require any knowledge of the phase of the form factor in experimentally inaccessible regions. Thus, the results of the present work are a rigorous consequence of the general principles and do not have any model dependence.

We start by giving in Sec. II a brief review of our theoretical framework. In Sec. III we present in detail the input quantities used in the application of the method to the K_{l3} form factors. In Sec. IV we review the main parameterizations used in the $K_{\ell 3}$ analyses, emphasizing the merits and the shortcomings of each of them. In Sec. V we concentrate on the parameterization based on the standard Taylor expansion at $t = 0$ and derive explicit constraints on the coefficients of the expansion. To facilitate further applications, we present the results as simple quadratic expressions for arbitrary input values of the form factors at special points inside the analyticity domain (the origin $t = 0$ and the Callan-Treiman(CT) point). For numerical illustrations, we use as input the precise values obtained recently from calculations in ChPT and on the lattice. We work in the isospin limit, but briefly discuss also the effects of symmetry breaking in Sec. V A. Further, in Sec. VI we investigate the truncation error related to the higher order terms in the expansion, and in Sec. VII we show that the method allows one to derive in a rigorous way the domains in the complex t -plane where zeros of the form factors are excluded. Sec. VIII contains some final remarks and our conclusions.

II. FORMALISM

A review of the formalism of unitarity bounds-in the standard version and the modified forms that include additional information on the unitarity cut- was given recently in [41]. Here we shall present for completeness the approach proposed in [42], which will be used in the applications made below.

We shall denote generically the form factors $f_+(t)$ and $f_0(t)$ by a function $F(t)$, which is real analytic in the complex t -plane except for the unitarity cut along the positive real axis from the lowest unitarity branch point $t_+ = (M_K + M_\pi)^2$ to ∞ . The dispersion relation satisfied by the correlator of two strangeness-changing vector currents (see details in Sec. III) implies an inequality of the type-

$$\int_{t_+}^{\infty} dt \rho(t)|F(t)|^2 \leq I, \quad (4)$$

where the weight function $\rho(t) \geq 0$ and the quantity I are known.

According to the Fermi-Watson theorem [22, 23], below the inelastic threshold t_{in} the phase of $F(t)$ is equal (modulo π) to the phase $\delta(t)$ of a partial wave of πK elastic scattering. Thus, we can write

$$F(t + i\epsilon) = |F(t)|e^{i\delta(t)}, \quad t_+ < t < t_{\text{in}}, \quad (5)$$

where $\delta(t)$ is known. We define the Omnès function

$$\mathcal{O}(t) = \exp\left(\frac{t}{\pi} \int_{t_+}^{\infty} dt' \frac{\delta(t')}{t'(t' - t)}\right), \quad (6)$$

where $\delta(t)$ is known for $t \leq t_{\text{in}}$ and is an arbitrary function, sufficiently smooth (*i.e.*, Lipschitz continuous) for $t > t_{\text{in}}$. From (5) and (6) it follows that the function

$$h(t) = F(t)[\mathcal{O}(t)]^{-1}, \quad (7)$$

has a larger analyticity domain, namely, the complex t -plane cut only for $t > t_{\text{in}}$. We further assume that a reliable parameterization of the modulus $|F(t)|$ is available on the same range $t_+ < t < t_{\text{in}}$, such that the quantity

$$I' = I - \int_{t_+}^{t_{\text{in}}} dt \rho(t)|F(t)|^2 \quad (8)$$

is known. Then from (4) we obtain an L^2 norm condition

$$\int_{t_{\text{in}}}^{\infty} dt \rho(t)|\mathcal{O}(t)|^2|h(t)|^2 \leq I' \quad (9)$$

for the function $h(t)$ analytic in the t -plane cut for $t > t_{\text{in}}$. As shown in [42], (9) can be brought into a canonical form by making the conformal transformation

$$\tilde{z}(t) = \frac{\sqrt{t_{\text{in}}} - \sqrt{t_{\text{in}} - t}}{\sqrt{t_{\text{in}}} + \sqrt{t_{\text{in}} - t}}, \quad (10)$$

which maps the complex t -plane cut for $t > t_{\text{in}}$ onto the unit disk in the z -plane defined by $z = \tilde{z}(t)$. Then, (9) can be written as

$$\frac{1}{2\pi} \int_0^{2\pi} d\theta |g(\exp(i\theta))|^2 \leq I', \quad (11)$$

where the function $g(z)$ is defined as

$$g(z) = w(z) \omega(z) F(\tilde{t}(z)) [\mathcal{O}(z)]^{-1}. \quad (12)$$

In this relation, $\tilde{t}(z)$ is the inverse of $z = \tilde{z}(t)$, for $\tilde{z}(t)$ defined in (10) and $w(z)$ is an outer function, *i.e.*, a function analytic and without zeros in $|z| < 1$, whose modulus on the boundary is related to the weight $\rho(t)$ and the Jacobian of the transformation (10) by

$$\frac{|w(\exp(i\theta))|^2}{2\pi} = \rho(\tilde{t}(\exp(i\theta))) \left| \frac{d\tilde{t}(\exp(i\theta))}{d\theta} \right|, \quad (13)$$

In general, an outer function is obtained from its modulus on the boundary by the integral

$$w(z) = \exp \left[\frac{1}{2\pi} \int_0^{2\pi} d\theta \frac{e^{i\theta} + z}{e^{i\theta} - z} \ln |w(e^{i\theta})| \right], \quad (14)$$

but in simple cases one can obtain an analytic form (see Sec. III D). Further, the function $O(z)$ is defined as

$$O(z) = \mathcal{O}(\tilde{t}(z)), \quad (15)$$

and

$$\omega(z) = \exp \left(\frac{\sqrt{t_{\text{in}} - \tilde{t}(z)}}{\pi} \int_{t_{\text{in}}}^{\infty} dt' \frac{\ln |\mathcal{O}(t')|}{\sqrt{t' - t_{\text{in}}}(t' - \tilde{t}(z))} \right). \quad (16)$$

From the definition (12), taking into account (7), it follows that $g(z)$ is analytic within the unit disc $|z| < 1$. The relation (11) leads to constraints on the values of g and its derivatives at various points (mathematically, this is known as the Meiman problem). In the general case, consider the first K derivatives of $g(z)$ at $z = 0$ and the values at other N interior points z_n :

$$\begin{aligned} \left[\frac{1}{k!} \frac{d^k g(z)}{dz^k} \right]_{z=0} &= g_k, \quad 0 \leq k \leq K-1; \\ g(z_n) &= \xi_n, \quad z_n \neq 0, \quad 1 \leq n \leq N, \end{aligned} \quad (17)$$

where g_k and ξ_n are given numbers. Then the following determinantal inequality holds:

$$\begin{vmatrix} \bar{I} & \bar{\xi}_1 & \bar{\xi}_2 & \cdots & \bar{\xi}_N \\ \bar{\xi}_1 & \frac{z_1^{2K}}{1-z_1^2} & \frac{(z_1 z_2)^K}{1-z_1 z_2} & \cdots & \frac{(z_1 z_N)^K}{1-z_1 z_N} \\ \bar{\xi}_2 & \frac{(z_1 z_2)^K}{1-z_1 z_2} & \frac{(z_2)^{2K}}{1-z_2^2} & \cdots & \frac{(z_2 z_N)^K}{1-z_2 z_N} \\ \vdots & \vdots & \vdots & \ddots & \vdots \\ \bar{\xi}_N & \frac{(z_1 z_N)^K}{1-z_1 z_N} & \frac{(z_2 z_N)^K}{1-z_2 z_N} & \cdots & \frac{z_N^{2K}}{1-z_N^2} \end{vmatrix} \geq 0, \quad (18)$$

where

$$\bar{\xi}_n = \xi_n - \sum_{k=0}^{K-1} g_k z_n^k, \quad \bar{I} = I' - \sum_{k=0}^{K-1} g_k^2. \quad (19)$$

All the principal minors of the above matrix should also be nonnegative [33, 35].

The entries of the determinant (18) are related, by (12), to the derivatives $F^{(j)}(0)$, $j \leq K-1$ of $F(t)$ at $t = 0$, and the values $F(t(z_n))$, respectively. It should be noted that (18) covers also the case of values given at complex points: if one of the numbers t_n is complex, also the complex conjugate appears, say $t_{n+1} = t_n^*$, and we have $F(t(z_{n+1})) = F^*(t(z_n))$ due to the reality property. The same relations hold for the corresponding points in the z -plane and the values $g(z_n)$. This ensures the reality of the determinant appearing in the inequality (18).

We note that the formalism presented above exploits in an optimal way the relation (9), which is a consequence of the inequality (4) and of the relations (5)-(8). The standard approach [32, 33, 35, 37, 38], which does not include additional information on the form factors on the cut, is obtained formally from the above relations by setting $t_{\text{in}} \rightarrow t_+$, when both the Omnès function $O(t)$ and the function $\omega(z)$ become unity. The implementation of the phase condition (5) on the elastic cut, together with the relation (4), involves the solution of an integral equation of Fredholm type (for details and references, see [41]).

We stress that, while (9) is a necessary condition following from the original inequality (4), it is not sufficient for the fulfillment of (4), *i.e.*, functions that satisfy (9) and do not satisfy (4) may exist. In principle, both conditions must be imposed in order to restrict the allowed domain of the parameters of interest: each condition leads to an allowed domain, the final region being the intersection of the corresponding domains. As shown in [41], by a conservative choice of t_{in} , the results obtained from (9) satisfy also the condition (4). We shall place ourselves in this framework here. Finally, we recall that in the definition (6) of the Omnès function, the phase for $t > t_{\text{in}}$ is not specified and can be parameterized in an arbitrary way. As shown in [41], the results are independent of the form chosen, in particular of the phase at asymptotic energies, provided that the parametrization is sufficiently smooth (*i.e.* Lipschitz continuous).

III. APPLICATION TO THE K_{l3} FORM FACTORS

In this section we apply the above formalism to the K_{l3} form factors $f_+(t)$ and $f_0(t)$. We first write down dispersion relations for suitable QCD correlators and show how they lead to an inequality of the type (4). Then we briefly discuss the low-energy theorems and the information on the phase and modulus on the elastic part of the cut used as input. For completeness we give also the explicit form of the outer functions defined above. We work in the isospin limit, adopting the convention that M_K and M_π are the masses of the charged mesons. A few comments about isospin breaking effects will be made in Sec. V A.

A. QCD correlators

We consider the correlator of the strangeness-changing hadronic current $V^\nu = \bar{s}\gamma^\nu u$:

$$\begin{aligned} \Pi^{\mu\nu}(q) &\equiv i \int d^4x e^{iq \cdot x} \langle 0 | T \{ V^\mu(x) V^\nu(0)^\dagger \} | 0 \rangle \quad (20) \\ &= (-g^{\mu\nu} q^2 + q^\mu q^\nu) \Pi_1(q^2) + q^\mu q^\nu \Pi_0(q^2). \end{aligned}$$

In QCD, the invariant amplitudes satisfy subtracted dispersion relations. More exactly, it is convenient to define

the functions [35, 37, 38]¹

$$\chi_1(Q^2) \equiv -\frac{1}{2} \frac{\partial^2}{\partial(Q^2)^2} [Q^2 \Pi_1(-Q^2)], \quad (21)$$

$$\chi_0(Q^2) \equiv \frac{\partial}{\partial Q^2} [Q^2 \Pi_0(-Q^2)], \quad (22)$$

which satisfy the dispersion relations

$$\chi_1(Q^2) = \frac{1}{\pi} \int_0^\infty dt \frac{t \text{Im}\Pi_1(t)}{(t+Q^2)^3}, \quad (23)$$

$$\chi_0(Q^2) = \frac{1}{\pi} \int_0^\infty dt \frac{t \text{Im}\Pi_0(t)}{(t+Q^2)^2}. \quad (24)$$

Unitarity implies that the spectral functions are positive for $t > t_+$ and satisfy the inequalities [35, 38]:

$$\text{Im}\Pi_1(t) \geq \frac{3}{2} \frac{1}{48\pi} \frac{[(t-t_+)(t-t_-)]^{3/2}}{t^3} |f_+(t)|^2, \quad (25)$$

$$\text{Im}\Pi_0(t) \geq \frac{3}{2} \frac{t_+ t_-}{16\pi} \frac{[(t-t_+)(t-t_-)]^{1/2}}{t^3} |f_0(t)|^2, \quad (26)$$

with $t_\pm = (M_K \pm M_\pi)^2$.

In the limit $Q^2 \gg \Lambda_{QCD}^2$, the correlators $\chi_1(Q^2)$ and $\chi_0(Q^2)$ can be calculated by perturbative QCD. Recent calculations to order α_s^4 (see [44, 45] and references therein) give:

$$\begin{aligned} \chi_1(Q^2) &= \frac{1}{8\pi^2 Q^2} \left(1 + \frac{\alpha_s}{\pi} - 0.062\alpha_s^2 \right. \\ &\quad \left. - 0.162\alpha_s^3 - 0.176\alpha_s^4 \right), \end{aligned} \quad (27)$$

$$\begin{aligned} \chi_0(Q^2) &= \frac{3(m_s - m_u)^2}{8\pi^2 Q^2} \left(1 + 1.80\alpha_s + 4.65\alpha_s^2 \right. \\ &\quad \left. + 15.0\alpha_s^3 + 57.4\alpha_s^4 \right). \end{aligned} \quad (28)$$

We omitted the power corrections due to nonzero masses and QCD condensates, as they are negligible.

The relations (21)-(26) show that each form factor satisfies a relation of the type (4), where

$$\begin{aligned} \rho_+(t) &= \frac{1}{32\pi^2} \frac{[(t-t_+)(t-t_-)]^{3/2}}{t^2(t+Q^2)^3}, \\ \rho_0(t) &= \frac{3t_+ t_-}{32\pi^2} \frac{[(t-t_+)(t-t_-)]^{1/2}}{t^2(t+Q^2)^2}, \end{aligned} \quad (29)$$

and

$$I_+ = \chi_1(Q^2), \quad I_0 = \chi_0(Q^2). \quad (30)$$

We evaluated these expressions taking $Q^2 = 4 \text{ GeV}^2$ as in [37, 38], $m_s(2 \text{ GeV}) = 98 \pm 10 \text{ MeV}$, $m_u(2 \text{ GeV}) = 3 \pm 1 \text{ MeV}$ [3] and $\alpha_s(2 \text{ GeV}) = 0.308 \pm 0.014$, which results from the recent average $\alpha_s(m_\tau) = 0.330 \pm 0.014$ [46]. This gives $\chi_1(2 \text{ GeV}) = (343.8 \pm 51.6) \times 10^{-5} \text{ GeV}^{-2}$ and $\chi_0(2 \text{ GeV}) = (253 \pm 68) \times 10^{-6}$.

B. Low-energy theorems

The theorems based on symmetries at low energies provide useful ingredients in the applications of the above formalism. At $t = 0$ by construction one has $f_0(0) = f_+(0)$, since $f_-(t)$ is regular at $t = 0$, and SU(3) symmetry implies $f_+(0) = 1$. Deviations from this limit are expected to be small [16] and have been calculated in chiral perturbation theory [17, 47] and more recently on the lattice (see the reviews in [1]-[5]). In the case of the scalar form factor, current algebra relates the value of the scalar form factor at the CT point $\Delta_{K\pi} \equiv M_K^2 - M_\pi^2$ to the ratio F_K/F_π of the decay constants [18, 19]:

$$f_0(\Delta_{K\pi}) = F_K/F_\pi / + \Delta_{CT}. \quad (31)$$

To one-loop in ChPT in the isospin limit $\Delta_{CT} = -3.1 \times 10^{-3}$ [21]. Results on higher-order corrections, and also beyond the isospin limit, are available [5, 47, 48].

At $\bar{\Delta}_{K\pi} (= -\Delta_{K\pi})$, a soft-kaon result [20] relates the value of the scalar form factor to F_π/F_K

$$f_0(-\Delta_{K\pi}) = F_\pi/F_K + \bar{\Delta}_{CT}. \quad (32)$$

A calculation in ChPT to one-loop in the isospin limit [21] gives $\bar{\Delta}_{CT} = 0.03$, but the higher order ChPT corrections are expected to be larger in this case. The estimate made in [30] leads to a rather large allowed interval for $\bar{\Delta}_{CT}$.

In the present work we use as input the values of the vector and scalar form factor at $t = 0$. For the scalar form factor we impose also the value $f_0(\Delta_{K\pi})$ at the first CT point. As discussed in [40], due to the poor knowledge of $\bar{\Delta}_{CT}$, the low-energy theorem (32) is not useful for further constraining the shape of the $K_{\ell 3}$ form factors at low energies.

For generality, we shall present our results for arbitrary values of the parameters $f_+(0)$ and $f_0(\Delta_{K\pi})$. For the numerical illustration of the results we shall use as default the values

$$f_+(0) = 0.962 \pm 0.005, \quad f_0(\Delta_{K\pi}) = 1.193 \pm 0.006. \quad (33)$$

The central value of $f_+(0)$ coincides practically with the ChPT prediction given in [17] and is quoted in [1] as the most recent lattice result. A slightly different average of lattice results $f_+(0) = 0.959 \pm 0.005$ is also quoted in [1]. The value of $f_0(\Delta_{K\pi})$ is consistent with the values reported in the review [1] in the isospin limit.

¹ The choice of the renormalization-group invariant correlators is not unique. Alternative definitions and the corresponding dispersion relations are shown to lead to almost identical constraints for the $K_{\ell 3}$ form factors [43]. Here we consider for convenience only the correlators (21) and (22).

The value (31) at the first CT point is quite precise in the standard model(SM). On the other hand, it has been suggested that deviations from ChPT at both CT points would be a signature for physics beyond the SM, such as right-handed quark couplings to W^\pm and charged Higgs [2, 29, 49]. In what follows, we shall derive constraints on the expansion coefficients both with, and without the condition at the CT point. We shall also derive a relation that correlates the values of the scalar form factor at $t = 0$ and at both CT points, which acts as an independent constraint for specific models beyond SM.

C. Phase and modulus on the elastic region of the cut

We recall that the first inelastic threshold for the scalar form factor is set by the $K\eta$ state, and for the vector form factor by the state $K^*\pi$, which suggests we take $t_{\text{in}} = (1 \text{ GeV})^2$. Strictly speaking, we must consider the inelasticity due to $K\pi\pi\pi$ at $(0.91 \text{ GeV})^2$, but its influence is considered weak and may be neglected. Moreover, it is known that the elastic region extends practically up to the $K\eta'$ threshold, which would justify the choice $t_{\text{in}} = (1.4 \text{ GeV})^2$. The analysis performed in [41] led to the conclusion that this choice overconstrains the system, at least for the scalar form factor. Therefore, in this work we make the conservative choice $t_{\text{in}} = (1 \text{ GeV})^2$ for both the scalar and vector form factors.

Below t_{in} the function $\delta(t)$ entering (6) is the phase of the S -wave of $I = 1/2$ of the elastic $K\pi$ scattering for the scalar form factor, and the phase of the P -wave of $I = 1/2$ for the vector form factor. In our calculations we used as default below t_{in} the phases from [28, 50] for the scalar form factor, and from [27, 30] for the vector case (the differences between the two phases were taken as an estimate of the uncertainty related to this input; see [40]). We recall that, while the standard dispersion approaches require a choice of the phase above t_{in} , the present formalism is independent of this ambiguity [41]. Above t_{in} we have taken $\delta(t)$ as a smooth function approaching π at high energies. As we mentioned in Sec. II, the results are independent of the choice of the phase for $t > t_{\text{in}}$. We have checked numerically this independence with high precision.

To estimate the low-energy integral in (8), we used the Breit-Wigner parameterizations of $|f_+(t)|$ and $|f_0(t)|$ in terms of the resonances given by the Belle Collaboration [24] for fitting the rate of $\tau \rightarrow K\pi\nu$ decay. This leads to the value $31.4 \times 10^{-5} \text{ GeV}^{-2}$ for the vector form factor and 60.9×10^{-6} for the scalar form factor. By combining with the values of $I_{+,0}$ defined in (30), we obtain

$$I'_+ = (312 \pm 69) \times 10^{-5} \text{ GeV}^{-2}, \quad I'_0 = (192 \pm 90) \times 10^{-6}. \quad (34)$$

Note that we use the Breit-Wigner parameterizations of $|f_{+,0}(t)|$ obtained in [24] only for estimating the low-energy integral appearing in (8). The parameterizations are

not extrapolated outside the resonance region; therefore their analytic properties do not play a role in the present formalism, where the analyticity of the form factors is exactly imposed. We note also that the dependence on the modulus information below t_{in} is very mild, as it is used only for the computation of the low-energy part of the integral (4). In fact, the results depend rather weakly on the values of $I'_{+,0}$, and moreover the dependence is monotonic: an increase of these quantities leads to more conservative bounds.

In our earlier work, [40] we had carried out an analysis on the uncertainties to be attached to our determination associated with the uncertainties of the inputs. This was essential as the rather high choice of t_{in} of $(1.4 \text{ GeV})^2$. Having chosen for this work the conservative choice of $(1 \text{ GeV})^2$, partly motivated by the considerations of our later work [41], we have obtained the new constraints that comfortably accommodate the prior results, including the uncertainties. Therefore, we consider only the results based on the central values of the input on the unitarity cut.

D. Outer functions

The outer function is defined in (13). Using (10) and (29), a straightforward calculations leads to

$$w_+(z) = \frac{1}{8\sqrt{2\pi t_{\text{in}}}} \sqrt{1-z^2} \quad (35) \\ \times \frac{(1+\tilde{z}(-Q^2))^3}{(1-z\tilde{z}(-Q^2))^3} \frac{(1-z\tilde{z}(t_+))^{3/2}(1-z\tilde{z}(t_-))^{3/2}}{(1+\tilde{z}(t_+))^{3/2}(1+\tilde{z}(t_-))^{3/2}},$$

for the vector form factor, and

$$w_0(z) = \frac{\sqrt{3}(M_K^2 - M_\pi^2)}{16\sqrt{2\pi t_{\text{in}}}} \sqrt{1-z} (1+z)^{3/2} \quad (36) \\ \times \frac{(1+\tilde{z}(-Q^2))^2(1-z\tilde{z}(t_+))^{1/2}(1-z\tilde{z}(t_-))^{1/2}}{(1-z\tilde{z}(-Q^2))^2(1+\tilde{z}(t_+))^{1/2}(1+\tilde{z}(t_-))^{1/2}},$$

for the scalar form factor. Here, z is the current variable and $\tilde{z}(t)$ is the function defined in (10). The outer functions for the standard version [35, 37, 38] are obtained from the above by replacing t_{in} with t_+ .

IV. PARAMETERIZATIONS OF $K\ell_3$ FORM FACTORS

The first parameterizations used simple pole models describing the t -dependence of $f_+(t)$ and $f_0(t)$ in terms of the lightest vector and scalar resonances with masses M_v and M_s , respectively:

$$f_+(t) = f_+(0) \frac{M_v^2}{M_v^2 - t}, \quad f_0(t) = f_0(0) \frac{M_s^2}{M_s^2 - t}. \quad (37)$$

The increase of the precision of the $K\ell_3$ experiments required more effective parameterizations.

A. Taylor expansions

The simplest expressions, adopted in practically all the experimental analyses [6]-[13], are based on the Taylor expansion around the point $t = 0$:

$$\hat{f}_+(t) = 1 + \sum_{k=1}^{K-1} c_{k,+} t^k, \quad \hat{f}_0(t) = 1 + \sum_{k=1}^{K-1} c_{k,0} t^k, \quad (38)$$

where $\hat{f}_{+,0}(t) = f_{+,0}(t)/f_+(0)$. The first coefficients are often expressed in terms of dimensionless slope and curvature:

$$c_1 = \frac{\lambda'}{M_{\pi^+}^2}, \quad c_2 = \frac{\lambda''}{2 M_{\pi^+}^4}, \quad (39)$$

which are also related by $\lambda' = M_{\pi^+}^2 \langle r_{\pi K}^2 / 6 \rangle$ and $\lambda'' = 2 M_{\pi^+}^4 c$ to the radius squared $\langle r_{\pi K}^2 \rangle$ and curvature c used in some papers [17, 37, 39].

The Taylor expansions converge in the disc $|t| < t_+$ limited by the first unitarity branch point. Therefore, in the semileptonic range $M_l^2 \leq t \leq t_-$, the convergence is expected to be rather good, with the asymptotic rate $t_-/t_+ = 0.31$. Of course, the convergence becomes poor if the expansions are used outside the $K_{\ell 3}$ region.

At the present experimental accuracy, only a few coefficients c_k can be determined from the data (common choices are $K = 2$ or $K = 3$). A theoretical correlation between the coefficients would be helpful in fitting the data with more parameters. The formalism discussed here is a useful tool in this sense. In the next section, we shall derive strong correlations between the slope and curvature defined in (39). Also, we will show how to obtain a bound on a suitably defined truncation error, which reflects the influence of the neglected higher order terms in the expansions (38).

B. Dispersive parameterization

Recently, NA48 [12], KLOE [13], and KTeV [14] Collaborations reanalyzed their data with a dispersive representation of the Omnès type, proposed in [29, 30]. The parameterizations of the two $K_{\ell 3}$ form factors read:

$$\begin{aligned} f_+(t) &= f_+(0) \exp \left[\frac{t}{M_\pi^2} (\lambda_+ + H(t)) \right], \\ f_0(t) &= f_+(0) \exp \left[\frac{t}{M_K^2 - M_\pi^2} (\ln[C] - G(t)) \right], \end{aligned} \quad (40)$$

where λ_+ is the slope of the vector form factor, $\ln[C] = \ln[f_0(M_K^2 - M_\pi^2)]$ is the logarithm of the scalar form factor at the CT point and the functions $H(t)$ and $G(t)$ are dispersive integrals upon the phases $\delta_{+,0}(t)$ of the form factors.

The advantage of this type of parameterization is that it includes information on the analytic properties of the form factors in the complex plane and on the phase,

known (modulo $\pm\pi$) in the elastic region $t < t_{\text{in}}$ from low-energy $K\pi$ phases. However, at larger energies the phase is not known, and this introduces an ambiguity in the representation. At infinity, the phase approaches a constant, whose value depends on the number of zeros of the form factor [30, 51], so as to ensure the asymptotic decrease like $1/t$ required by perturbative QCD [52].

Actually, the dispersion relations (40) require only one subtraction. In order to display the free parameters λ'_+ and C , an additional subtraction was performed, at $t = 0$ and $t = \Delta_{K\pi}$, respectively. This reduces the dependence on the unknown $\delta(t)$ above t_{in} , but at the same time spoils the asymptotic behavior of the form factors (see [53] for a discussion in a similar context). The correct behavior can be restored only by imposing additional sum rules, which in general are not easy to implement in the fitting procedure.

As noted above, the representations (40) assume that the form factors do not have zeros in the complex plane. The influence of possible zeros, analyzed in [30], depends on their position in the complex plane. Information about the presence of the zeros at low energies is therefore important for the dispersive representations mentioned here. In Sec. VII we shall derive rigorous domains where zero values of the form factors are excluded.

C. z -parameterizations

A class of parameterizations used alternatively for various weak form factors are based on expansions in powers of a variable that maps conformally the t -plane onto a disk. For the $K\pi$ form factors the method was discussed in [38] and more recently was used by the KTeV Collaboration to reanalyze their $K_{\ell 3}$ data [11].

The expansion is actually based on the method of unitarity bounds discussed in the present paper. Consider the standard version, based only on the inequality (4), without information on the phase and modulus on the unitarity cut. In this case, as discussed at the end of Sec. II, one should replace t_{in} by t_+ when $I' = I$ and the functions $O(t)$ and $\omega(z)$ defined in (6) and (16), respectively, are equal to unity. Then, referring for illustration to the vector form factor, from (12) one can write the representation

$$f_+(t) = \frac{1}{w_+(z)} \sum_{k=0}^{\infty} g_k z^k, \quad (41)$$

where

$$w_+(z) = \frac{\sqrt{1-z^2}}{32\sqrt{\pi t_+}} \frac{(1+\bar{z}(-Q^2))^3 (1-z\bar{z}(t_-))^{3/2}}{(1-z\bar{z}(-Q^2))^3 (1+\bar{z}(t_-))^{3/2}}. \quad (42)$$

Here $z = \bar{z}(t)$, where

$$\bar{z}(t) = \frac{\sqrt{t_+} - \sqrt{t_+ - t}}{\sqrt{t_+} + \sqrt{t_+ - t}}. \quad (43)$$

An advantage of the z -expansion is that it allows one to derive a bound on the truncation error, describing the effect of the neglected higher order terms in the expansion [38]. On the other hand, from (42) it follows that the outer function vanishes at $z = \pm 1$, points that by (43) correspond to t_+ and infinity in the t -plane, respectively. The zeros in the denominator are not compensated automatically if the sum in the numerator of (41) is truncated at a finite order. Therefore, the representation (41) has unphysical singularities at the threshold t_+ and at infinity. These deficiencies of the standard z -expansion were discussed in the similar case of the $B\pi$ form factor in [53], where alternative z -expansions free of such singularities were investigated. Such parameterizations are useful and deserve further study also for the $K_{\ell 3}$ form factors.

V. CONSTRAINTS ON THE EXPANSION COEFFICIENTS

In this section we consider the most common parameterization of the $K_{\ell 3}$ form factors based on the Taylor expansions (38). This parameterization does not include in an explicit way information on the analytic properties of the form factors and their behavior on the unitarity cut. However, the mathematical method reviewed in Sec. II allows one to derive constraints on the expansion coefficients, which follow from these properties. One improves in this way the quality of the expansion, which includes in an implicit way additional theoretical information.

Using as input the value of I'_+ given in (34) and the phase and modulus below $t_{\text{in}} = (1 \text{ GeV})^2$ described in Sec. III, we obtain from (18) the following constraint on the slope λ'_+ and curvature λ''_+ of the vector form factor, for an arbitrary $f_0 \equiv f_+(0)$:

$$f_0^2[(\lambda''_+)^2 - 0.107\lambda'_+\lambda''_+ + 2.18 \times 10^{-4}\lambda''_+ + 2.98 \times 10^{-3}(\lambda'_+)^2 - 1.49 \times 10^{-5}\lambda'_+ + 4.20 \times 10^{-8}] - 4.67 \times 10^{-7} \leq 0. \quad (44)$$

The numerical coefficients of this relation depend on the phase in the elastic region and the coefficient I'_+ defined in (34), which gives the last term in the left hand side of the inequality.

As an illustration, for the input value $f_+(0) = 0.962$ given in (33), the inequality (44) is represented as the interior of the smallest ellipse in the slope-curvature plane in Fig. 1. The alternative input $f_+(0) = 0.959$ adopted in [1] leads to practically the same ellipse. For completeness, we represent in the same figure the domains obtained using as input the normalization at $t = 0$ and the standard unitarity bounds, without information on the phase and modulus (the largest ellipse), and the domain obtained by including in the standard unitarity bounds the phase on the elastic region, known from the Fermi-Watson theorem (the intermediate ellipse). The small ellipse is situated inside the other two, which confirms that all the constraints are satisfied by the domain described by the inequality (44).

In Fig. 2, the constraint (44) is represented together with experimental points from [4, 8, 9, 12–15], where we have extracted the corresponding curvature from the constrained fit given in [13]. We note that, except the results from NA48 and KLOE, which have curvatures slightly larger than the allowed values, the experimental data satisfy the constraints. We note also that the theoretical predictions $\lambda'_+ = (24.9 \pm 1.3) \times 10^{-3}$, $\lambda''_+ = (1.6 \pm 0.5) \times 10^{-3}$ obtained from ChPT to two loops [5], and $\lambda'_+ = (26.05^{+0.21}_{-0.51}) \times 10^{-3}$, $\lambda''_+ = (1.29^{+0.01}_{-0.04}) \times 10^{-3}$ [27], and $\lambda'_+ = (25.49 \pm 0.31) \times 10^{-3}$, $\lambda''_+ = (1.22 \pm 0.14) \times 10^{-3}$ [31] obtained from dispersion relations are consistent with the constraint: the expression in the left side of (44) is negative when evaluated with $f_+(0) = 0.962$ and the central values of the slope and curvature given above.

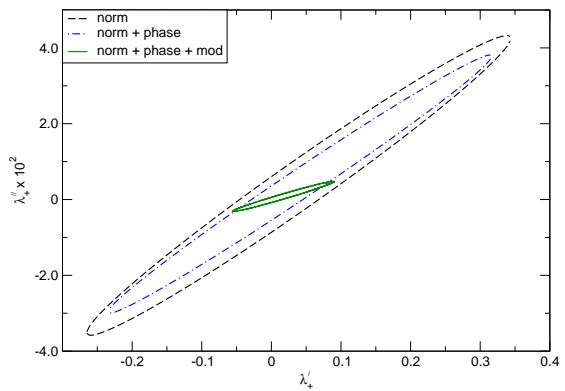


FIG. 1: Allowed domain for the slope and curvature of the vector form factor, using the normalization $f_+(0) = 0.962$ and phase and modulus information up to $t_{\text{in}} = (1 \text{ GeV})^2$.

The analogous constraint for the slope and curvature of the scalar form factor for an arbitrary normalization $f_0 \equiv f_+(0)$ reads:

$$f_0^2[(\lambda''_0)^2 - 0.059\lambda'_0\lambda''_0 - 3.58 \times 10^{-4}\lambda''_0 + 9.72 \times 10^{-4}(\lambda'_0)^2 + 9.64 \times 10^{-6}\lambda'_0 + 3.67 \times 10^{-8}] - 8.05 \times 10^{-8} \leq 0. \quad (45)$$

In deriving this constraint, we used the value of I'_0 from (34) and the phase and modulus described in Sec. III. For illustration, for $f_0 = 0.962$ we obtain the small ellipse in Fig. 3 where, as in Fig. 1, the larger ellipses are obtained using the standard unitarity bounds. These constraints are satisfied by the points in the domain (45).

If we include in addition the constraint at the first CT point, $f_{CT} \equiv f_0(\Delta_{K\pi})$, we obtain the inequality

$$f_0^2[(\lambda''_0)^2 + 0.25\lambda'_0\lambda''_0 + 21.6 \times 10^{-3}\lambda''_0 + 15.3 \times 10^{-3}(\lambda'_0)^2 + 2.68 \times 10^{-3}\lambda'_0 + 1.17 \times 10^{-4}] - 10^{-3}f_0f_{CT}(2.67\lambda'_0 + 21.53\lambda''_0 + 0.23) + 1.16 \times 10^{-4}f_{CT}^2 - 3.23 \times 10^{-10} \leq 0. \quad (46)$$

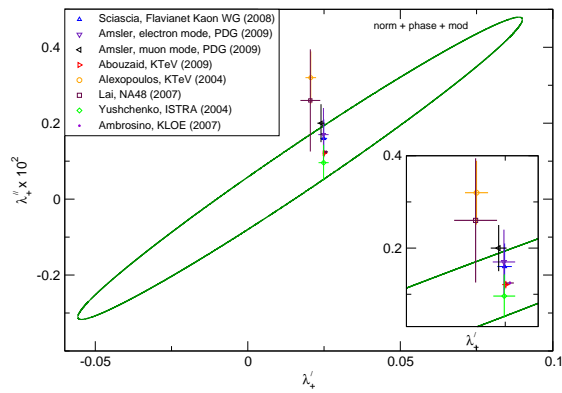


FIG. 2: The best constraints for the slope and curvature of the vector form factor for $f_+(0) = 0.962$ compared with experimental determinations.

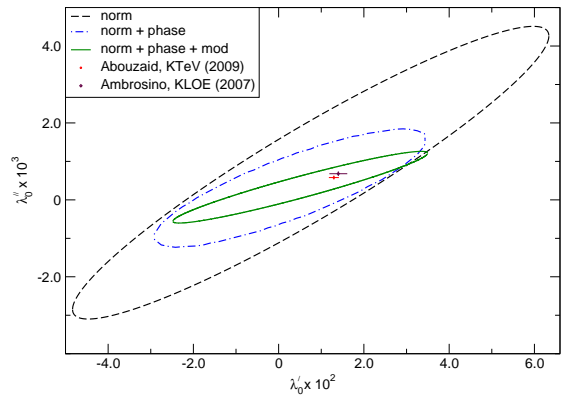


FIG. 3: Allowed domain for the slope and curvature of the scalar form factor, using as input the normalization $f_+(0) = 0.962$ and phase and modulus information up to $t_{\text{in}} = (1 \text{ GeV})^2$.

For the central values given in (33), this domain is the interior of the small ellipse in Fig. 4. The large ellipse in this figure represents the allowed domain obtained from the standard unitarity bounds with the same input at interior points, and the intermediate ellipse is obtained from the standard unitarity bounds by imposing also the phase below t_{in} according to the Fermi-Watson theorem. The small ellipse is situated inside the other two, which shows that the slope and the curvature which satisfy the inequality (46) obey also the standard unitarity bounds.

The above domains were obtained for the central values of the parameters in (33). As shown in [40], the inclusion of uncertainties in the inputs has the effect of slightly enlarging the allowed domains. In particular, there is a straightforward dependence of the shape of the ellipses on

the input I' . These could be subject to uncertainties both in pQCD as well as due to the uncertainties in modelling the modulus information. However, the resulting ellipses simply shrink or expand if I' is taken to be smaller or larger.

We note that the theoretical prediction of ChPT to two loops $\lambda'_0 = (13.9^{-0.4}_{+1.3} \pm 0.4) \times 10^{-3}$, $\lambda''_0 = (8.0^{-1.7}_{+0.3}) \times 10^{-4}$ reported in [5] is consistent within errors with the constraint (46) with the default input (33): for the central value of the slope λ'_0 given above, the range of λ''_0 allowed by (46) is $(8.24 \times 10^{-4}, 8.42 \times 10^{-4})$. The same is true for the theoretical prediction $\lambda'_0 = (16.00 \pm 1.00) \times 10^{-3}$, $\lambda''_0 = (6.34 \pm 0.38) \times 10^{-4}$ obtained in [26] from dispersion relations.

As concerns the experimental values, Figs. 3 and 4 show that the determinations [13] (we have extracted the curvature from the constrained fit therein) and [14] are consistent with the phase and modulus information together with the normalization (33), but are outside the domain obtained when we impose also the CT theorem, with the input value given in (33).

In Fig. 5, we compare the allowed bands for the slope λ'_0 , corresponding to the end points of the ellipses defined by the inequalities (45) and (46) for the same input as above, with the experimental determinations. As noted already, the slope predicted by NA48 [7] is not consistent with the SM input at $t = 0$ and $t = \Delta_{K\pi}$. This conclusion is very stable with respect to the input value of I'_0 , which gives the last term in the l.h.s. of (46): it turns out that only by increasing this value by a factor of almost 5, the allowed ellipse is inflated enough as to include the central value of the slope from [7]. The relation (46) implies also that, keeping I'_0 and $f_+(0)$ fixed, one must reduce the input value at the CT point down to $f_+(\Delta_{K\pi}) = 1.138$ in order to have the central value of the slope from [7] inside the allowed domain.

We end this section on the shape of the K_{l3} form factors with a comment on the low-energy theorem (32) at the second CT point. As discussed in Sec. III B, due to the poor knowledge of the correction $\bar{\Delta}_{CT}$, this theorem does not constrain further the coefficients of the expansion beyond the domain obtained with the input at $t = 0$ and $t = \Delta_{K\pi}$. On the other hand, using these values as input, the formalism presented in Sec. II leads to an allowed domain for the value of the scalar form factor at $t = -\Delta_{K\pi}$. Namely, from the proper input in the determinant (18) we obtain the inequality

$$0.177\bar{f}_{CT}^2 + 0.086f_{CT}^2 + 0.523f_0^2 - 0.425f_0f_{CT} - 0.608f_0\bar{f}_{CT} + 0.246f_{CT}\bar{f}_{CT} - 1.92 \times 10^{-4} \leq 0, \quad (47)$$

where $\bar{f}_{CT} \equiv f_0(-\Delta_{K\pi})$. This relation correlates the values of the scalar form factor at $t = 0$ and at the two CT points and represents a nontrivial analyticity constraint for the predictions beyond the SM. As shown in [40], for the input values (33), the inequality (47) leads to a narrow range $-0.046 \leq \bar{\Delta}_{CT} \leq 0.014$ for the correction defined in (32), improving the ChPT prediction reported

in [30].

A. Isospin breaking effects

The bounds given above were obtained in the limit of isospin symmetry. We recall that in our convention M_K and M_π are the masses of the charged mesons. As discussed recently [5], the isospin breaking effects should be taken into account at the present level of experimental and theoretical precision. At low energy, at next-to-leading order in the chiral expansion, there are strong isospin violations at order $(m_d - m_u)p^2$ and electromagnetic corrections at order $e^2 p^2$, while the next-to-next-to-leading order terms include corrections up to order $(m_d - m_u)^2 p^4$.

In the formalism considered here, isospin symmetry was used in the unitarity relations (25) and (26), where the matrix elements of the $K^+\pi^0$ and $K^0\pi^+$ pairs entering the unitarity sum were related by symmetry. The description of the form factors on the unitarity cut in terms of resonances suggests that the isospin corrections in this region are small (for a detailed discussion see [27]). So, the unitarity relations (25) and (26) and, consequently, the outer functions defined in Sec. III D conserve their form. We checked also that a change of about 0.02 rad of the phase below t_{in} , suggested to represent isospin effects [30], leaves the results practically unmodified.

If the symmetry is broken, one must use the physical pion and kaon masses in the evaluation of the unitarity threshold and the phase space factors. To illustrate this effect, we recalculated the constraints (44)-(46) using the same input on the unitarity cut, with the exception of M_π , taken to be the mass of the neutral pion. For instance, we obtain instead of (46) the inequality

$$\begin{aligned} f_0^2 [(\lambda_0'')^2 + 0.24\lambda_0'\lambda_0'' + 21.3 \times 10^{-3}\lambda_0'' + 15.1 \times 10^{-3}(\lambda_0')^2 \\ + 2.62 \times 10^{-3}\lambda_0' + 1.14 \times 10^{-4}] - 10^{-3}f_0f_{CT}(2.61\lambda_0' \\ + 21.23\lambda_0'' + 0.23) + 1.13 \times 10^{-4}f_{CT}^2 - 3.21 \times 10^{-10} \leq 0, \end{aligned} \quad (48)$$

where the definition of the slope and curvature is still based on the mass of the charged pion, as in (38). The small differences between (46) and (48) are due to the fact that the position of the CT point and its image in the z -plane are slightly changed if the pion mass is modified.

The inequality (48) can be used to constrain the slope and curvature for the $K^+\pi^0$ form factor using the isospin corrections for the same form factor at $t = 0$ and the CT point [5, 48]. For instance, by increasing simultaneously the values given in (33), $f_+(0)$ by 2% [48] and $f_0(\Delta_{K\pi})$ by 0.029 [5, 48], we obtain from (48) an ellipse slightly shifted towards the right by the amount $\delta\lambda_0' \approx 0.0007$ compared to the small ellipse in Fig. 4. The shifted ellipse leads to curvatures slightly higher for the same slope than those obtained in the isospin limit.

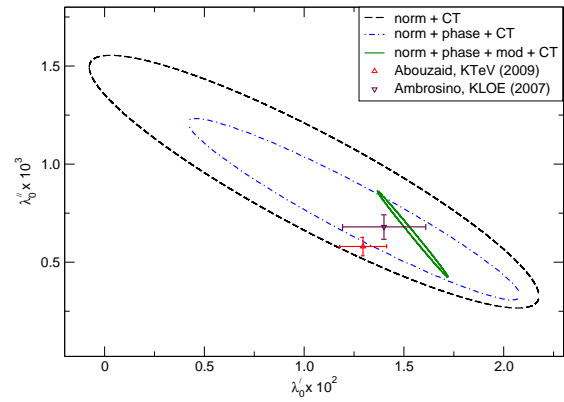


FIG. 4: Allowed domain for the slope and curvature of the scalar form factor, using the normalization $f_+(0) = 0.962$, the value $f_0(\Delta_{K\pi}) = 1.193$, and phase and modulus information up to $t_{\text{in}} = (1 \text{ GeV})^2$.

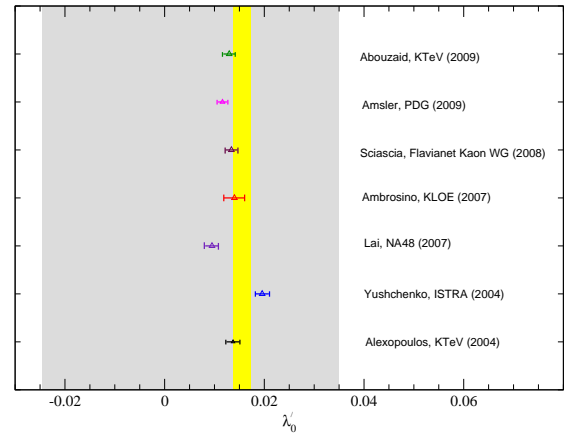


FIG. 5: Allowed bands for the slope of the scalar form factor obtained from (45) large band, and (46) narrow band, for $f_+(0) = 0.962$ and $f_0(\Delta_{K\pi}) = 1.193$, compared with the experimental information.

VI. BOUNDS ON THE TRUNCATION ERROR

One might ask how accurate is the representation of the $K_{\ell 3}$ form factors in the physical region by a few terms in the Taylor expansion (38). It is also of interest to know the extrapolation error if the truncated expansion is used beyond the physical region up to, say, the CT point $t = \Delta_{K\pi}$. To answer these questions one needs an estimate of the higher-order terms neglected in usual parameterizations. As discussed in previous works, for instance [36], [38], [53], the technique of unitarity bounds allows one to find a model-independent estimate of the theoretical error produced by the truncation of the Taylor

expansion.

We assume that the fit provides values of the coefficients c_k , for $k \leq K-1$, in the truncated expansion (38). Since the series is convergent in the physical region, one expects the influence of the higher terms to be gradually smaller. We recall that, asymptotically, the convergence rate scales as t/t_+ , where t_+ is the convergence radius, and this ratio does not exceed 0.31 in the semileptonic region.

Following, for instance, the suggestion made in [53], one can define the truncation error as the first term neglected in the expansion:

$$\delta\hat{f}_{+,0}(t)_{\text{trunc}} \sim |c_K t^K|. \quad (49)$$

As further suggested in [53], it is reasonable to increase the number of terms until the truncation error becomes smaller than the experimental one.

Without additional information, it is in general impossible to estimate the magnitude of higher terms in an expansion, even if it is convergent. Fortunately, in the present case, using the fundamental inequality (18) of Sec. II and the relation (12) between the function g and the form factor F , it is possible to derive upper and lower bounds on the next coefficient c_K in terms of the coefficients c_k , supposed to be known for $k \leq K-1$.

For illustration, we give below the constraint relating the value $f_0 \equiv f_+(0)$, the slope λ' and the curvature λ'' , to the next coefficient c_3 . For the vector form factor the relation is

$$\begin{aligned} & f_0^2[c_3^2 + c_3(-0.045 + 79.2\lambda'_+ - 4953.4\lambda''_+) \\ & + 1892.5(\lambda'_+)^2 - 3.39\lambda'_+ - 2.07 \times 10^5\lambda'_+\lambda''_+ + 134.45\lambda''_- \\ & + 6.24 \times 10^6(\lambda''_+)^2 + 5.1 \times 10^{-3}] - 0.051 \leq 0, \end{aligned} \quad (50)$$

while the similar relation for the scalar form factor, without imposing the CT theorem, reads

$$\begin{aligned} & f_0^2[c_3^2 + c_3(-0.29 + 8.41\lambda'_0 - 3321.5\lambda''_0) \\ & + 123.2(\lambda'_0)^2 - 0.18\lambda'_0 - 2.04 \times 10^4\lambda'_0\lambda''_0 + 445.9\lambda''_- \\ & + 2.87 \times 10^6(\lambda''_0)^2 + 0.025] - 0.0087 \leq 0. \end{aligned} \quad (51)$$

The numerical coefficients in these inequalities depend on the particular dispersion relation satisfied by the QCD correlators, their perturbative expressions, and the information on the phase and modulus on the elastic part of the cut.

As a numerical example, let us take for the vector form factor the central values $\lambda'_+ = 25.09 \times 10^{-3}$ and $\lambda''_+ = 1.21 \times 10^{-3}$ [14]. Then, for our choice $f_0(0) = 0.962$, we obtain from (50) the allowed interval $1.79 \text{ GeV}^{-6} \leq c_3 \leq 2.25 \text{ GeV}^{-6}$, which implies a correction at the end of the semileptonic region $\delta\hat{f}_+(t_-)$ between 3.5×10^{-3} and 4.4×10^{-3} .

For the scalar form factor, taking a point $\lambda'_0 = 15 \times 10^{-3}$ and $\lambda''_0 = 0.69 \times 10^{-3}$, situated inside the small ellipses in Figs. 3 and 4, we obtain from (51) the range

$1.14 \text{ GeV}^{-6} \leq c_3 \leq 1.32 \text{ GeV}^{-6}$, which implies a correction $\delta\hat{f}_0(t_-)$ at the end of the semileptonic region between 2.2×10^{-3} and 2.5×10^{-3} . On the other hand, evaluated at the CT point, the term $c_3 t^3$ produces a correction of about 0.014 to $f_0(\Delta_{K\pi})$, larger than the error quoted in (33). So, even for a quadratic parameterization of the scalar form factor, the extrapolation to the CT point is not precise enough for testing possible deviations from the SM. Of course, in practical applications one should use in (50) and (51) the values of the slope and curvature obtained from the fits of the data.

We note that the relations (50) and (51) are useful also if one uses a cubic parameterization in the experimental analysis. In this case, the relations provide theoretical constraints for the next coefficient c_3 included in the fit. The truncation error can then be estimated using a constraint on the next coefficient c_4 , which is obtained in a straightforward way from the general relation (18).

VII. DOMAINS WHERE ZEROS ARE EXCLUDED

The question of the zeros of the form factors is important from theoretical and practical points of view. The dispersive representations of the Omnès type require the knowledge of the zeros in the complex plane. The zeros are important also in ChPT, where their presence is required in some cases by symmetry arguments [51, 54].

A study of the zeros of the pion electromagnetic form factor was performed in [55]. For the $K\pi$ form factors, the influence of possible zeros in the context of Omnès dispersive representations has been analyzed in [30]. The absence of zeros is assumed in the recent analysis of KTeV data reported in [14].

The mathematical techniques presented in Sec. II can be adapted in a straightforward way to the problem of zeros. Let us assume that the form factor $F(t)$ has a simple zero on the real axis, $F(t_0) = 0$. From the relation (12) it follows that $g(z_0) = 0$, where $z_0 = \tilde{z}(t_0)$. We shall use this information in the determinant condition (18): if the zero is compatible with the remaining information, the inequality (18) can be satisfied. If, on the contrary, the inequality is violated, the zero is excluded. It follows that we can obtain from (18) a rigorous condition for the domain of points z_0 (or t_0) where the zeros are excluded. First assume that we use as input only the value of the form factor at $t = 0$. Then from (18) the domain is given by

$$\begin{vmatrix} I' - g_0^2 & -g_0 \\ -g_0 & \frac{\tilde{z}(t_0)^2}{1-\tilde{z}(t_0)^2} \end{vmatrix} \leq 0. \quad (52)$$

Here, I' is defined in (8), g_0 is related to the value $F(0)$ by the relation (12), and $\tilde{z}(t)$ is defined in (10). If we include in addition the value of the form factor at some point t_1 (for instance, $t_1 = \Delta_{K\pi}$ for the scalar form factor), the condition reads:

$$\begin{vmatrix} I' - g_0^2 & g(\tilde{z}(t_1)) - g_0 & -g_0 \\ g(\tilde{z}(t_1)) - g_0 & \frac{\tilde{z}(t_1)^2}{1-\tilde{z}(t_1)^2} & \frac{\tilde{z}(t_1)\tilde{z}(t_0)}{1-\tilde{z}(t_1)\tilde{z}(t_0)} \\ -g_0 & \frac{\tilde{z}(t_1)\tilde{z}(t_0)}{1-\tilde{z}(t_1)\tilde{z}(t_0)} & \frac{\tilde{z}(t_0)^2}{1-\tilde{z}(t_0)^2} \end{vmatrix} \leq 0. \quad (53)$$

To illustrate the method we use the default input $f_+(0) = 0.962$ and $f_0(\Delta_{K\pi}) = 1.193$. Then, from (52) it follows that in the case of the vector form factors, simple zeros are excluded in the interval $-0.31 \text{ GeV}^2 \leq t_0 \leq 0.23 \text{ GeV}^2$ of the real axis, while for the scalar form factor the range with no zeros is $-0.91 \text{ GeV}^2 \leq t_0 \leq 0.48 \text{ GeV}^2$. If we also impose the low-energy theorem (31), with the value of $f_0(\Delta_{K\pi})$ from (33), the condition (53) implies that the scalar form factor cannot have simple zeros in the range $-1.81 \text{ GeV}^2 \leq t_0 \leq 0.93 \text{ GeV}^2$. The formalism rules out zeros in the physical region of the kaon semileptonic decay.

We have also studied the sensitivity of the variation of our inputs. The dependence on the parametrizations of the scattering phase shifts; the uncertainties in $f_+(0)$ and $f_0(\Delta_{K\pi})$ are found to be imperceptible. On the other hand, the uncertainties on the quantity I'_+ given in (34) lead to the following limits for the region where zeros are excluded for the vector form factors: $-0.28 \text{ GeV}^2 \leq t \leq 0.22 \text{ GeV}^2$ for the maximum value and $-0.36 \text{ GeV}^2 \leq t \leq 0.26 \text{ GeV}^2$ for the minimum value. The corresponding limits for the scalar form factor upon inclusion of the constraint from the CT points from the uncertainties in I'_0 , quoted in (34), are: $-1.60 \text{ GeV}^2 \leq t \leq 0.91 \text{ GeV}^2$ and $-2.26 \text{ GeV}^2 \leq t \leq 0.97 \text{ GeV}^2$ respectively.

The method can be easily extended to the case of complex zeros. Since the functions are real analytic, *i.e.* they satisfy the relation $F(t^*) = F^*(t)$, the zeros appear in complex conjugate pairs: if $F(t_0) = 0$, then also $F(t_0^*) = 0$. We can implement this condition by formally setting in (53) $t_1 \rightarrow t_0^*$ and $g(\tilde{z}(t_1)) \rightarrow 0$. So, the complex domain where zeros are excluded by the normalization at $t = 0$ is given by

$$\begin{vmatrix} I' - g_0^2 & -g_0 & -g_0 \\ -g_0 & \frac{\tilde{z}(t_0^*)^2}{1-\tilde{z}(t_0^*)^2} & \frac{\tilde{z}(t_0^*)\tilde{z}(t_0)}{1-\tilde{z}(t_0^*)\tilde{z}(t_0)} \\ -g_0 & \frac{\tilde{z}(t_0^*)\tilde{z}(t_0)}{1-\tilde{z}(t_0^*)\tilde{z}(t_0)} & \frac{\tilde{z}(t_0)^2}{1-\tilde{z}(t_0)^2} \end{vmatrix} \leq 0. \quad (54)$$

The determinant can be generalized in a straightforward way to include an additional interior point, such as the CT point for the scalar form factor. The corresponding domains are given in Figs. 6-8. On the real axis, the figures indicate the points where double zeros are excluded. The small domains are obtained without including information on the phase and modulus on the unitarity cut. As discussed in Sec. II, this case is obtained formally by replacing t_{in} by t_+ .

As in the case of the real zeros, the issue of the stability of the exclusion regions of complex zeros is an important

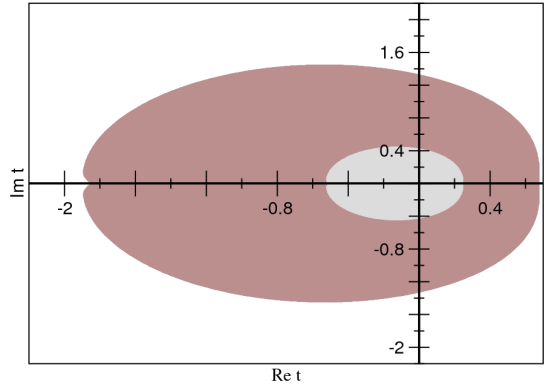


FIG. 6: Domain where zeros of the vector form factor are excluded, derived from (54). The small domain is obtained without including phase and modulus in the elastic region.

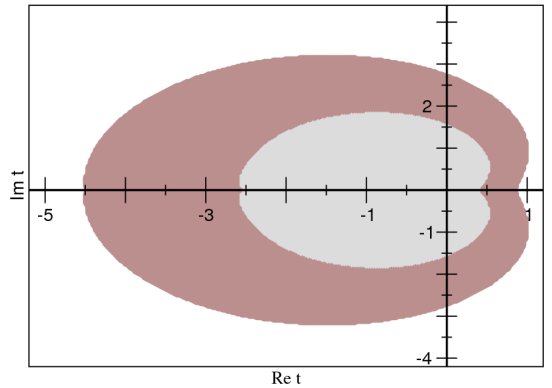


FIG. 7: Domain without zeros for the scalar form factor, derived from (54) for $f_+(0) = 0.962$. The small domain is obtained without including phase and modulus in the elastic region.

one against variations of the inputs. Here, too, the main uncertainty stems from those of I'_+ and I'_0 . The results of these are shown in Figs. 9 and 10.

We emphasize that our method is able to give in a rigorous way the regions where zeros are excluded, but says nothing about the remaining regions. Thus, we cannot answer the question whether the zeros are excluded everywhere, or a zero must exist. We recall that we applied a formalism that exploits a necessary condition, (9), which follows from (4), the Fermi-Watson theorem, and the knowledge of the modulus in the elastic region. Therefore, the violation of this condition is sufficient to ensure that the zero is not allowed.

A. Phenomenological consequences

Our results show that the zeros are excluded in a rather large domain at low energies. This provides confidence in the semiphenomenological analyses based on Omnes

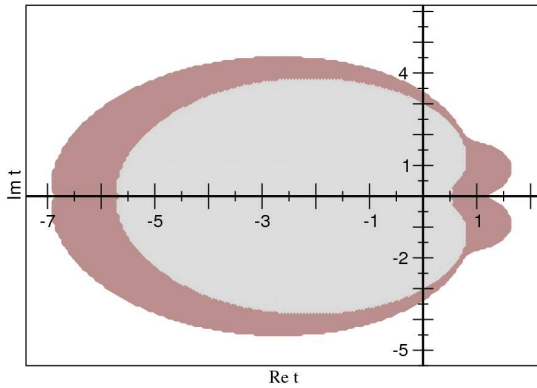


FIG. 8: As in Fig. 7, using in addition the input $f_0(\Delta_{K\pi}) = 1.193$.

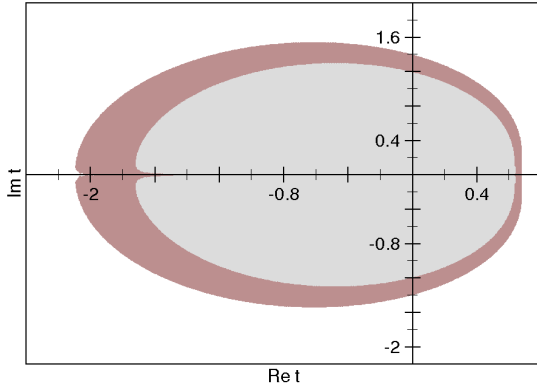


FIG. 9: Domains where zeros of the vector form factor are excluded, derived from (54), using $f_+(0) = 0.962$ and phase and modulus information up to $t_{in} = 1 \text{ GeV}^2$, when I'_+ is varied within the errors. The small (large) domain is obtained with the maximum (minimum) value of I'_+ given in (34).

representations, like those proposed in [29, 30], which assume that the zeros are absent. Indeed, a zero of the scalar form factor at -0.1 GeV^2 , which would distort the shape at low energies [30], is ruled out by our results. On the other hand, as shown in [30], a real zero at -1 GeV^2 leads already to a phenomenological form factor very similar to one with no zeros. This value is close to the extremity of -0.91 GeV^2 of the range without zeros for the scalar form factor, and the inclusion of the additional constraint at the CT point rules out a zero even at -1 GeV^2 . In the case of complex zeros as well, the allowed zeros are rather remote to produce visible effects: for instance, a pair of complex zeros located at $t_0 = (0.1 \pm 2i) \text{ GeV}^2$, considered in [30], is ruled out by our results.

In the case of the vector form factor, the analysis made in [30] using data from τ decay concludes that complex zeros cannot be excluded, due to the lack of information on the phase of the form factor in the inelastic region. In contrast, as shown in Fig. 6, the formalism presented here leads without any assumptions to a rather large domain where complex zeros are excluded. The stability

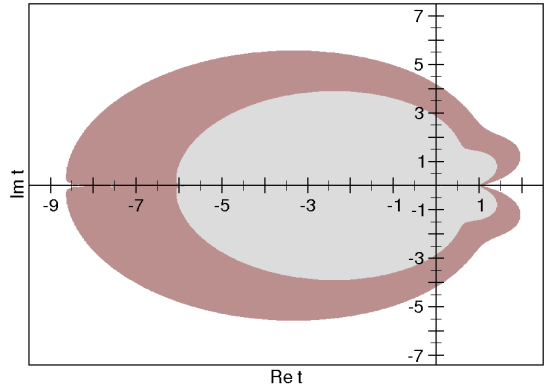


FIG. 10: Domains where zeros of the scalar form factor are excluded, derived using $f_+(0) = 0.962$, $f_0(\Delta_{K\pi}) = 1.193$, and phase and modulus information up to $t_{in} = 1 \text{ GeV}^2$, when I'_0 is varied within the errors. The small (large) domain is obtained with the maximum (minimum) value of I'_0 given in (34).

analysis shows that, although for the maximum values of I'_+ and I'_0 from (34) the domains do shrink, the implications for the phenomenological analyses are unchanged.

VIII. CONCLUSIONS

In this work we have studied the shape of the scalar and vector form factors in the $K\ell_3$ domain, crucial for the determination of the modulus of the CKM matrix element $|V_{us}|$. We applied a formalism proposed in [42], which develops the standard method of unitarity bounds by including in an optimal way the phase and the modulus on the elastic part of the unitarity cut. The formalism is also suitable for including information from soft-meson theorems at points inside the analyticity domain.

The work reported here is a detailed application of the techniques explored in [40], also wiring in the constraint to t_{in} explored in [41], to the phenomenology of the kaon semileptonic decay. It uses the powerful modified formalism for unitarity bounds and constraints from low-energy theorems. It goes beyond explorations of [39] which does not use phase and modulus information, or [37] which does not use modulus information for the scalar form factors. Here, the vector form factor is analyzed using the modified formalism which has never been done before. The modified formalism is employed to isolate those regions of the real energy line and complex energy plane where zeros are forbidden. Thus, this work represents a powerful application of the theory of unitarity bounds, which relies not so much on experimental information, but on theoretical inputs from perturbative QCD. It provides a powerful consistency check on determinations of shape parameters from phenomenology and experimental analyses. It may be noted that in the context of $B \rightarrow D^* l \bar{\nu}$ the dispersive bounds obtained in [56] were successfully used by experimental groups studying the

decay.

The method exploits analyticity and unitarity, but differs in several respects from the usual dispersion relations. In applying these relations, some assumptions about the form factor above the inelastic threshold are necessary. Moreover, in the Omnès-type representations it is assumed that the form factors have no zeros in the complex plane. No such assumptions are necessary in our approach. Instead, one exploits a dispersion relation for a QCD correlator, which is calculated perturbatively in the Euclidian region and is related by unitarity to the modulus squared of the form factors in the Minkowskian region. Positivity of the spectral functions then leads to an integral relation of the form (4) for the modulus squared of the form factor, which is the basic relation of the approach. From such a relation one cannot make definite predictions for the values of the form factors or their derivatives, but only derive bounds on these values. On the other hand, a remarkable feature is that an arbitrary number of values can be included simultaneously, corresponding mathematically to the so-called Meiman problem. Thus, the formalism is very useful for finding correlations between the values of the form factors at different points and for testing the consistency of inputs known from different sources on different regions of the complex plane.

In this work, we have focused on the phenomenological consequences of the formalism. We have considered the standard parameterization of the scalar and vector form factors in the $K_{\ell 3}$ physical region, based on the Taylor expansion at $t = 0$, and derived constraints on the coefficients of the expansion. The results for the slope and curvature are given in simple analytic form in Eqs. (44)-(46) for arbitrary values of $f_+(0)$ and $f_0(\Delta_{K\pi})$. The numerical coefficients in these inequalities depend on the dispersion relation satisfied by the QCD correlators, their perturbative expressions, and the input phase and modulus on the elastic part of the cut. The sensitivity of the coefficients to the uncertainty of the input is quite low, as shown in [40].

The constraints (44)-(46) can be used in the experimental fits with quadratic polynomials, or for testing *a posteriori* the consistency of the fitted parameters with theoretical information from regions outside the $K_{\ell 3}$ range. For illustration, the small ellipses in Figs. 1-4 represent these domains for the default input (33). The allowed values also satisfy the standard bounds and the phase condition in the elastic region, being included in the larger ellipses in the figures.

A more general condition, which correlates the coefficients of a cubic Taylor expansion, is given in Eqs. (50) and (51) for the vector and scalar form factors, respectively. These relations can be used either to estimate the truncation error of the quadratic expansions, or for constraining the fits based on a cubic parameterization.

We have worked in the isospin limit, but have also given a brief discussion of isospin breaking effects. The relation (48), obtained using the mass of the neutral pion

instead of the charged one, allows one to correlate the isospin corrections in the slope and curvature of the scalar $K^+\pi^0$ form factor to those at $t = 0$ and $t = \Delta_{K\pi}$.

We have also considered two other applications of the formalism: in (47) we have derived a relation between the values of the scalar form factor at the first and the second CT points, for an arbitrary $f_+(0)$. This represents a non-trivial analyticity constraint for the predictions beyond the SM suggested in [2, 29, 49]. We have studied also the possible zeros of the form factors, and have shown that they are excluded in a rather large domain at low energies for both the vector and the scalar form factors. The results support the recent dispersive representations of the Omnès type, which assume that the zeros are absent.

Finally, we point out that alternative expansions, for instance, in powers of the variable z defined in Sec. IV C, may be more convenient from the point of view of convergence than the standard Taylor parameterizations (38). Constraints on the coefficients of such expansions can be derived using similar techniques, and will be investigated in a future work.

Acknowledgement: BA thanks the Department of Science and Technology, Government of India, and the Homi Bhabha Fellowships Council for support. IC acknowledges support from CNCSIS in the Program Idei, Contract No. 464/2009, and from the National Authority for Scientific Research , Project No. PN-09370102. We thank S. Ramanan for discussions and collaboration at an early stage of this project, and V. Bernard and E. Passemard for discussions and for their careful reading of and comments on the manuscript.

[1] FlaviaNet Working Group on Kaon Decays, M. Antonelli *et al.* arXiv:1005.2323 [hep-ph].

[2] E. Passemar, PoS **KAON09**, 024 (2009) [arXiv:1003.4696 [hep-ph]].

[3] L. Lellouch, PoS **LATTICE2008** (2009) 015 [arXiv:0902.4545 [hep-lat]].

[4] B. Sciascia [FlaviaNet Kaon Working Group], Nucl. Phys. Proc. Suppl. **181-182**, 83 (2008) [arXiv:0812.1112 [hep-ex]].

[5] A. Kastner and H. Neufeld, Eur. Phys. J. C **57**, 541 (2008) [arXiv:0805.2222 [hep-ph]].

[6] A. Lai *et al.* [NA48 Collaboration], Phys. Lett. B **604**, 1 (2004) [arXiv:hep-ex/0410065].

[7] A. Lai *et al.* [NA48 Collaboration], Phys. Lett. B **647**, 341 (2007) [arXiv:hep-ex/0703002].

[8] O. P. Yushchenko *et al.*, Phys. Lett. B **581**, 31 (2004) [arXiv:hep-ex/0312004].

[9] T. Alexopoulos *et al.* [KTeV Collaboration], Phys. Rev. D **70**, 092007 (2004) [arXiv:hep-ex/0406003].

[10] F. Ambrosino *et al.* [KLOE Collaboration], Phys. Lett. B **636**, 166 (2006) [arXiv:hep-ex/0601038].

[11] E. Abouzaid *et al.* [KTeV collaboration], Phys. Rev. D **74**, 097101 (2007) [arXiv:hep-ex/0608058].

[12] A. Lai *et al.* [NA48 Collaboration], Phys. Lett. B **647**, 341 (2007) [arXiv:hep-ex/0703002].

[13] F. Ambrosino *et al.* [KLOE Collaboration], JHEP **0712**, 105 (2007) [arXiv:0710.4470 [hep-ex]].

[14] E. Abouzaid *et al.* [KTeV collaboration], Phys. Rev. D **81**, 052001 (2010) [arXiv:0912.1291 [hep-ex]].

[15] C. Amsler *et al.* [Particle Data Group], Phys. Lett. B **667**, 1 (2008).

[16] M. Ademollo and R. Gatto, Phys. Rev. Lett. **13**, 264 (1964).

[17] H. Leutwyler and M. Roos, Z. Phys. C **25**, 91 (1984).

[18] C. G. Callan and S. B. Treiman, Phys. Rev. Lett. **16**, 153 (1966).

[19] R. F. Dashen and M. Weinstein, Phys. Rev. Lett. **22**, 1337 (1969).

[20] R. Oehme, Phys. Rev. Lett. **16**, 215 (1966).

[21] J. Gasser and H. Leutwyler, Nucl. Phys. B **250**, 517 (1985).

[22] K. M. Watson, Phys. Rev. **95**, 228 (1954).

[23] E. Fermi, Nuovo Cim. **2S1**, 17 (1955) [Riv. Nuovo Cim. **31**, 1 (2008)].

[24] D. Epifanov *et al.* [Belle Collaboration], Phys. Lett. B **654**, 65 (2007) [arXiv:0706.2231 [hep-ex]].

[25] M. Jamin, J. A. Oller and A. Pich, Nucl. Phys. B **622**, 279 (2002) [arXiv:hep-ph/0110193].

[26] M. Jamin, J. A. Oller and A. Pich, JHEP **0402**, 047 (2004) [arXiv:hep-ph/0401080].

[27] B. Moussallam, Eur. Phys. J. C **53**, 401 (2008) [arXiv:0710.0548 [hep-ph]].

[28] B. El-Bennich, A. Furman, R. Kaminski, L. Lesniak, B. Loiseau and B. Moussallam, Phys. Rev. D **79**, 094005 (2009) [arXiv:0902.3645 [hep-ph]].

[29] V. Bernard, M. Oertel, E. Passemar and J. Stern, Phys. Lett. B **638**, 480 (2006) [arXiv:hep-ph/0603202].

[30] V. Bernard, M. Oertel, E. Passemar and J. Stern, Phys. Rev. D **80**, 034034 (2009) [arXiv:0903.1654 [hep-ph]].

[31] D. R. Boito, R. Escribano and M. Jamin, JHEP **1009**, 031 (2010) [arXiv:1007.1858 [hep-ph]].

[32] S. Okubo, Phys. Rev. D **3**, 2807 (1971).

[33] V. Singh and A. K. Raina, Fortsch. Phys. **27**, 561 (1979).

[34] G. Auberson, G. Mahoux and F. R. A. Simao, Nucl. Phys. B **98**, 204 (1975).

[35] C. Bourrely, B. Machet and E. de Rafael, Nucl. Phys. B **189**, 157 (1981).

[36] R.F. Lebed and K. Schilcher, Phys. Lett.B **430**, 341 (1998) [arXiv:hep-ph/9710489].

[37] C. Bourrely and I. Caprini, Nucl. Phys. B **722**, 149 (2005) [arXiv:hep-ph/0504016].

[38] R. J. Hill, Phys. Rev. D **74**, 096006 (2006) [arXiv:hep-ph/0607108].

[39] G. Abbas and B. Ananthanarayan, Eur. Phys. J. A **41**, 7 (2009) [arXiv:0905.0951 [hep-ph]].

[40] G. Abbas, B. Ananthanarayan, I. Caprini, I. Sentitemsu Imsong and S. Ramanan, Eur. Phys. J. A **44**, 175 (2010) [arXiv:0912.2831 [hep-ph]].

[41] G. Abbas, B. Ananthanarayan, I. Caprini, I. S. Imsong and S. Ramanan, Eur. Phys. J. A **45**, 389 (2010) arXiv:1004.4257 [hep-ph].

[42] I. Caprini, Eur. Phys. J. C **13**, 471 (2000) [arXiv:hep-ph/9907227].

[43] I. Caprini and E.M. Babalic, Rom. J. Phys. **55**, 920 (2010)

[44] P. A. Baikov, K. G. Chetyrkin and J. H. Kuhn, Phys. Rev. Lett. **96**, 012003 (2006) [arXiv:hep-ph/0511063].

[45] P. A. Baikov, K. G. Chetyrkin and J. H. Kuhn, Phys. Rev. Lett. **101**, 012002 (2008) [arXiv:0801.1821 [hep-ph]].

[46] S. Bethke, Eur. Phys. J. C **64**, 689 (2009) [arXiv:0908.1135 [hep-ph]].

[47] J. Bijnens and P. Talavera, Nucl. Phys. B **669**, 341 (2003) [arXiv:hep-ph/0303103].

[48] J. Bijnens, K. Ghorbani, arXiv:0711.0148 (2007).

[49] O. Deschamps, S. Descotes-Genon, S. Monteil, V. Niess, S. T'Jampens and V. Tisserand, arXiv:0907.5135 [hep-ph].

[50] P. Buettiker, S. Descotes-Genon and B. Moussallam, Eur. Phys. J. C **33**, 409 (2004) [arXiv:hep-ph/0310283].

[51] B. Ananthanarayan, I. Caprini, G. Colangelo, J. Gasser and H. Leutwyler, Phys. Lett. B **602**, 218 (2004) [arXiv:hep-ph/0409222].

[52] G.P. Lepage and S.J. Brodsky, Phys. Rev. D **22**, 2157 (1980).

[53] C. Bourrely, I. Caprini and L. Lellouch, Phys. Rev. D **79**, 013008 (2009) [arXiv:0807.2722 [hep-ph]].

[54] H. Leutwyler, arXiv:hep-ph/0212324.

[55] I. Raszillier, W. Schmidt and I. S. Stefanescu, J. Math. Phys. **17**, 1957 (1976).

[56] I. Caprini, L. Lellouch and M. Neubert, Nucl. Phys. B **530**, 153 (1998) [arXiv:hep-ph/9712417].